Adv. Theor. Appl. Mech., Vol. 1, 2008, no. 3, 141 - 154

Comparisons on Self-Synchronizations of a Vibratory Screener with Considering Different Exciter Parameters

Qingkai Han* and Bangchun Wen

School of Mechanical Engineering and Automation
Northeastern University, Shenyang, China
* qhan@mail.neu.edu.cn

Abstract

Self-synchronization principle is employed to achieve special processing tasks in ore milling industry, such as a vibratory screener. A multi-degree-of-freedom dynamical model of a vibratory screener is developed in the manuscript. The efforts of exciter's mass eccentric moment, motor torque, rotating friction moment on the synchronizations of the motion of the vibratory screener, including transient motion, are investigated through numerical simulations. In particular, when a driven motor is shut down, the possible continuity of the self-synchronization motion of the screener, called synchronous transmission, at certain conditions is investigated.

Keywords: Vibratory system, self-synchronization, exciter parameters, simulations

1 Introduction

The well known self-synchronization means of the in-time motions of two or more oscillating mechanical bodies, due to inner coupling constraints, which is on contrast to the controlled synchronization which need to introduce special controller actions [1].

Self-synchronization has received a lot of attentions for many kinds of vibratory machines, such as self-synchronous vibratory screeners, conveyers and so on [2]. The self-synchronization state of a vibratory machine, usually driven by two identical eccentric exciters, refers to the motion that the machine body vibrates in one main direction only, while the vibro-exciters' of the machine approach an identical speed. In order to achieve self-synchronous vibration, the two exciters with eccentric mass driven by two motors should be chosen and installed properly.

Because of the complexity of self-synchronization in the vibratory machinery, classical vibration theories are not adequate and effective in analyzing the system as shown in recent research [4, 5]. Therefore, stable harmonic responses have been widely assumed in simplified dynamical models of self-synchronous vibratory machines [3, 4]. As is widely acknowledged, a comprehensive study on self-synchronizations is important for many other fields associated with general mechanical systems [6, 7]. In this paper, the steady-state processes synchronization and transient processes of a vibratory screener with self-synchronous vibrations are investigated via numerical simulations. The effects of eccentric moment of exciters, motor out-torques, and eccentric motor's rotary friction moments on the synchronizations are investigated. An interesting phenomenon, that the system can maintain its synchronous motion even if one of the motors stops working after the synchronous vibration is realized, called synchronous transmission, is revealed.

2. Differential equations of a synchronous vibratory screener

2.1 Differential equations

As illustrated in a research by the authors [8], the photo of a self-synchronous vibratory screener with two eccentric exciters and its dynamical sketch are shown in Figure 1.

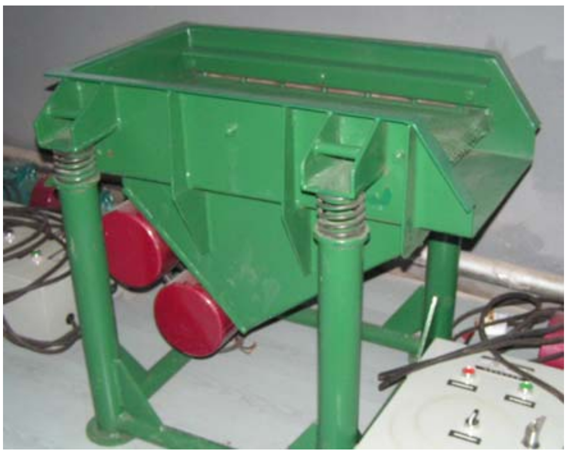

(a) Photo of a vibratory screener in laboratory, Type ZZS40-70

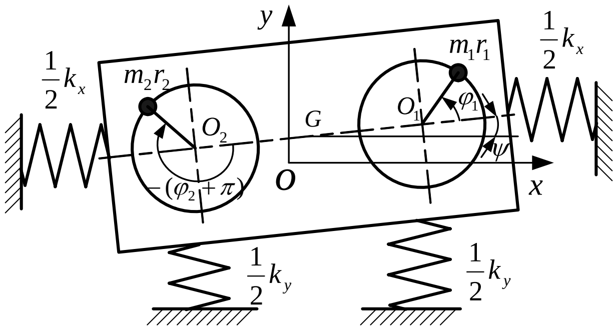

(b) Dynamical model

Figure 1. A self-synchronous vibratory screener with two exciters [8].

In the coordinate frame of *Oxy,* the differential equations of the vibratory screener are given as [8],

$$\boldsymbol{M}\ddot{\boldsymbol{X}} + \boldsymbol{C}\dot{\boldsymbol{X}} + \boldsymbol{K}\boldsymbol{X} = \boldsymbol{F}\,, \tag{1}$$

where, $\boldsymbol{X} = \{x \quad y \quad \psi \quad \varphi_1 \quad \varphi_2\}^T$, and x , y represent the horizontal and vertical displacements of the machine body; ψ is the swing angle of the body referring to its gravity center *G*; φ_1 and φ_2 are two rotating phase angles of the two exciters; $\boldsymbol{M}$, $\boldsymbol{C}$, $\boldsymbol{K}$ are the inertial matrix, damping coefficient matrix and stiffness matrix respectively, which are given [8],

$$\boldsymbol{M} = \begin{bmatrix} M & 0 & 0 & 0 & 0 \\ 0 & M & 0 & 0 & 0 \\ 0 & 0 & I & 0 & 0 \\ 0 & 0 & 0 & J_1 & 0 \\ 0 & 0 & 0 & 0 & J_2 \end{bmatrix}, \boldsymbol{C} = \begin{bmatrix} c_x & 0 & 0 & 0 & 0 \\ 0 & c_y & 0 & 0 & 0 \\ 0 & 0 & c & 0 & 0 \\ 0 & 0 & 0 & c_1 & 0 \\ 0 & 0 & 0 & 0 & c_2 \end{bmatrix}, \boldsymbol{K} = \begin{bmatrix} k_x & 0 & 0 & 0 & 0 \\ 0 & k_y & 0 & 0 & 0 \\ 0 & 0 & k_\phi & 0 & 0 \\ 0 & 0 & 0 & 0 & 0 \\ 0 & 0 & 0 & 0 & 0 \end{bmatrix} \tag{2}$$

where, $M = M_0 + m_1 + m_2$, M_0 is the mass of the machine body, and m_1, m_2 are the eccentric masses of the two exciters respectively; $I = I_0 + m_1 l^2 + m_2 l^2$, I_0 is the moment of inertia to its center *G*, l is the distance between two exciter rotors ($l = O_1O_2$); $J_i = m_i r_i^2$, $i = 1,\ 2$, is the moment of inertia of the two exciter rotors, r_i is the eccentric radius; c_x, c_y, c_ψ represent damping modulus in x, y, ψ of the machine body; $c = c_\psi + c_1 + c_2$, and c_1, c_2 represent the rotary damping modulus of the two eccentric rotors; k_x, k_y, k_ψ are the spring stiffness coefficients of machine body in x, y and ψ respectively.

In Eq. (1), $\boldsymbol{F}$ is the loading vector, which is

$$\mathbf{F} = \{f_1 \quad f_2 \quad f_3 \quad f_4 \quad f_5\}^T, \tag{3}$$

where, f_1, f_2, f_3 are the sum of the driving moments in every dofs of x, y, ψ, which are determined by eccentric mass, rotating speed and their fixed positions of the two exciters. f_4, f_5 are the driving moments of the two exciter rotors, which are determined by the driving motor characteristics, including output motor torques T_1 and T_2, eccentric mass, frictional moments, etc. All this forces are given as follows [8]:

$$f_1 = m_1 r_1 (\dot{\varphi}_1^2 \cos\varphi_1 + \ddot{\varphi}_1 \sin\varphi_1) - m_2 r_2 (\dot{\varphi}_2^2 \cos\varphi_2 + \ddot{\varphi}_2 \sin\varphi_2) + (m_1 - m_2) l (\ddot{\psi} \sin\psi + \dot{\psi}^2 \cos\psi),$$

$$f_2 = m_1 r_1 (\dot{\varphi}_1^2 \sin\varphi_1 - \ddot{\varphi}_1 \cos\varphi_1) + m_2 r_2 (\dot{\varphi}_2^2 \sin\varphi_2 - \ddot{\varphi}_2 \cos\varphi_2) - (m_1 - m_2) l (\ddot{\psi} \cos\psi - \dot{\psi}^2 \sin\psi),$$

$$f_3 = -(f_1\dot{\varphi}_1 - f_2\dot{\varphi}_2) + (m_1 - m_2) l (\ddot{x}\sin\psi - \ddot{y}\cos\psi) - m_1 r_1 l [\ddot{\varphi}_1 \cos(\varphi_1 - \psi) - \dot{\varphi}_1^2 \sin(\varphi_1 - \psi)] \\ + m_2 r_2 l [\ddot{\varphi}_2 \cos(\varphi_2 + \psi) - \dot{\varphi}_2^2 \sin(\varphi_2 + \psi)],$$

$$f_4 = T_1 - f_1\dot{\psi} - m_1 r_1 (\ddot{y}\cos\varphi_1 - \ddot{x}\sin\varphi_1) - m_1 r_1 l [\ddot{\psi}\cos(\varphi_1 - \psi) - \dot{\psi}^2 \sin(\varphi_1 - \psi)] - m_1 r_1 g \cos\varphi_1,$$

$$f_5 = T_2 + f_2\dot{\psi} - m_2 r_2 (\ddot{y}\cos\varphi_2 + \ddot{x}\sin\varphi_2) + m_2 r_2 l [\ddot{\psi}\cos(\varphi_2 + \psi) - \dot{\psi}^2 \sin(\varphi_2 + \psi)] - m_2 r_2 g \cos\varphi_2,$$

$$T_i = 2T_m s_m n_0 \frac{n_0 - n_i}{s_m^2 n_0^2 + (n_0 - n_i)^2}, \quad i = 1,\ 2 \tag{4}$$

where, n_0 is motors' normal speed; T_m is the maximum torque of motor, $T_m = K_T T_N$; s_m is the critical ratio of motor speed decreasing, $s_m = s_N (K_T + \sqrt{K_T^2 - 1})$; T_N, s_N, K_T are the rated torque, rated ratio of speed decreasing and the rated overload coefficient respectively. n_i is the rotating speed of motor.

2.2 Validation of the dynamical model

In the following simulations, the model parameters are selected according to the practical vibratory screener in laboratory as shown in Figure 1(a). The mass of the machine body in Eq. (1) is $M = 130\text{kg}$ and its rotating moment of inertia is $I = 33\text{kgm}^2$. The supporting stiffness of the machine body are $k_x = 30000\text{N/m}$, $k_y = 77600\text{N/m}$, and $k_\psi = 3000\text{Nm/rad}$. The masses of the two exciters are $m_1 = m_2 = 2.5\text{kg}$. The eccentric distances of the two exciters are $r_1 = r_2 = 0.08\text{m}$. The distance between the two exciters is $l = 0.4\text{m}$. The two identical motors' normal torques are $T_{\text{N1}} = T_{\text{N2}} = 2\text{Nm}$, and its rotating speed is $f_{\text{N}} = 16\text{Hz}$ with speed drawing ratio of $s_{\text{N1}} = s_{\text{N2}} = 5\%$ and mechanical ratio of $K_{\text{T1}} = K_{\text{T2}} = 2.5$. The approximate values of the damping coefficients of the system and exciter rotor are assumed as $c_x = c_y = 100\text{Ns/m}$, $c_\psi = 100\text{Nms/rad}$ for machine body, and $c_1 = c_2 = 0.01\text{Nms/rad}$ for the two rotating rotors of exciters, respectively.

These model parameters are validated firstly by experimental measurements of the screener, in which two acceleration sensors are used to measure the accelerations of the machine body in both horizontal and vertical directions. The measured vibrating acceleration in *x*-direction and its corresponding amplitude spectra are shown in Figure 2(a) and Figure 2(b) respectively, and the vibrating acceleration in y-direction and its spectra are shown in Figure 2(c) and (d). From the measured vibrations of the machine at the start of motion, it can be seen that the screener moves into its synchronization state after 4 seconds, while the acceleration amplitude in *x* direction are much smaller than that in *y* direction.

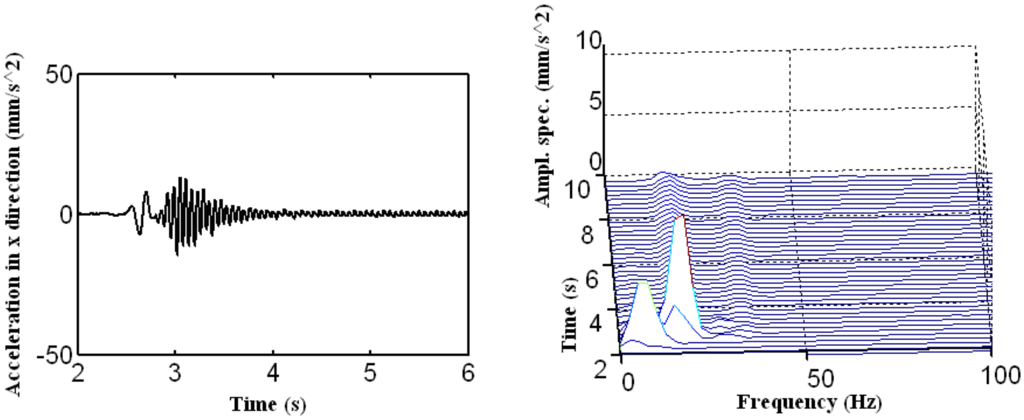

(a) The acceleration in *x* direction (b) 3D frequency spectra of acceleration in *x* direction

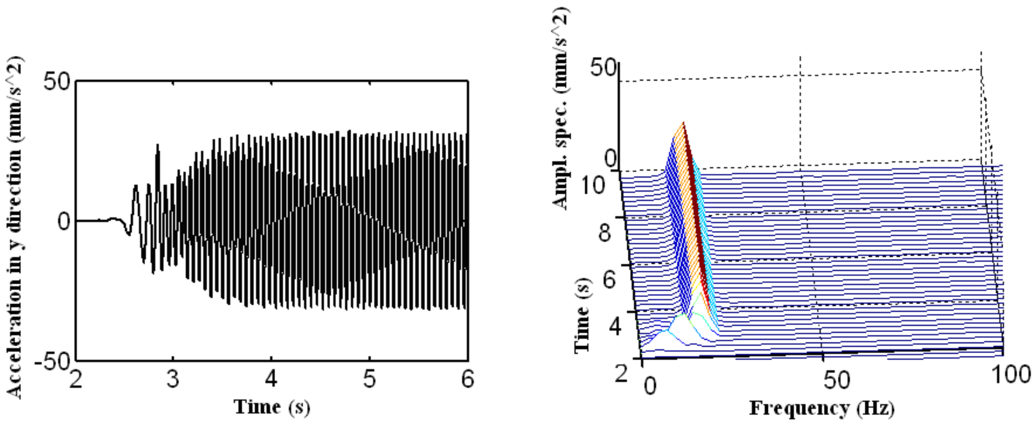

(c) The acceleration in *y* direction (d) 3D frequency spectra of acceleration in *y* direction

Figure 2. The measured accelerations of a vibratory screener.

Table 1 lists the comparison of amplitudes, derived from Eq. (1) and experimental measurements separately, of the machine body in x and y directions with fundamental frequency 1X, double frequency 2X, and the third-harmonics 3X, including the approximate stable periodical solutions. The stable solutions are resolved from Eq. (1) by assuming the average angular accelerations of the two motors being 0.

In order to make the model validation more general, initial phase angles of the two eccentric motors can be chosen by different values in simulations. Here, one of the motors is assumed with initial phase angle of 0, whilst another motor is with the initial phase angles of 0, 2, 5 rad. The motors' rotating frequency is 16 Hz.

As can be seen from the Table 1, the results based on the model are in good agreement with those from experiments indicating the effusiveness of the model.

Table 1 Comparisons of analytical stable solution, measured data and simulated results of the vibratory screener

Data sources	Motor initial phase (rad)		Amplitude in *x* direction (mm)			Amplitude in *y* direction (mm)		
	φ_1	φ_2	16 Hz	32 Hz	48Hz	16 Hz	32 Hz	48Hz
Stable periodic solution	—		0	0	0	2.85	0	0
	0	0	0	0	0	2.67	0.030	0.020
Simulation results	0	2	0	0	0	2.66	0.031	0.012
	0	5	0	0	0	2.67	0.0037	0.015
Experimental results	—		0.069	0.030	0.005	2.73	0.017	0.019

3 The effects of exciter's parameters on self-synchronous vibrations of screener

Once the model shown in Eq. (1) is verified from experimental data, numerical simulations are carried out to show how the effect of system parameters on the self-synchronous vibrations.

3.1 The exciters' eccentric moments

When the eccentric moments of the two exciters are $m_1r_1 = m_2r_2$ =0.2kgm, Figure 3(a) shows the simulated displacement in *x* direction of the machine body with its transient process. Figure 3(b) and 3(c) show the displacements in y direction and the body swing angle ψ around its gravity center respectively, while Figure 3(d), (e), (f) show the displacement *x*, displacement *y* and body swing angle ψ for the condition of $m_1r_1 = m_2r_2$ =0.4kgm, respectively.

Our results show that when the two exciters' eccentric moments increase from $m_1 r_1 = m_2 r_2$ =0.08, 0.2, to 0.32kgm, the increased stable synchronous vibrating amplitudes are 1.35mm, 2.67mm, 3.98mm corresponding. However, when the eccentric moments exceed a certain value, such as $m_1 r_1 = m_2 r_2$ =0.4kgm, it is found that the vibrating system cannot realize a self-synchronous movement. In addition, all vibrations in the dimensions of x, y and ψ of the machine body are large and do not decrease at all over a long period. As a result, the machine vibrates with low frequencies, and the phase angle differences of two motors will keep on increasing leading to unstable state.

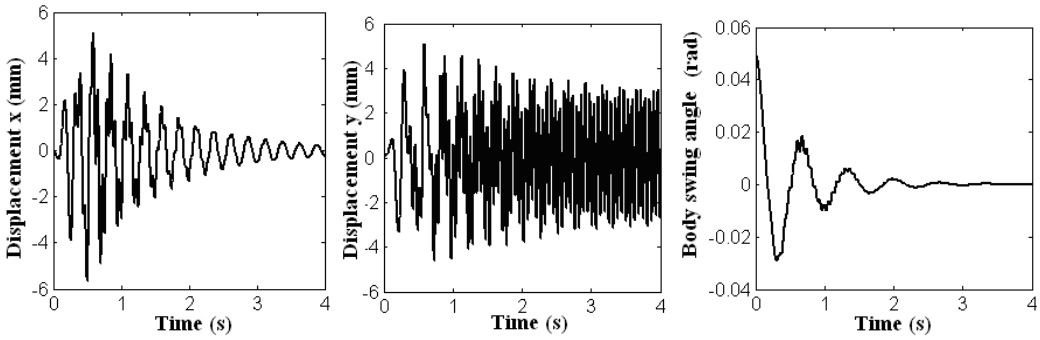

(a) Displacement *x* for $m_i r_i$ =0.2kgm (b) Displacement *y* for $m_i r_i$ =0.2kgm (c) Body swing angle for $m_i r_i$ =0.2kgm

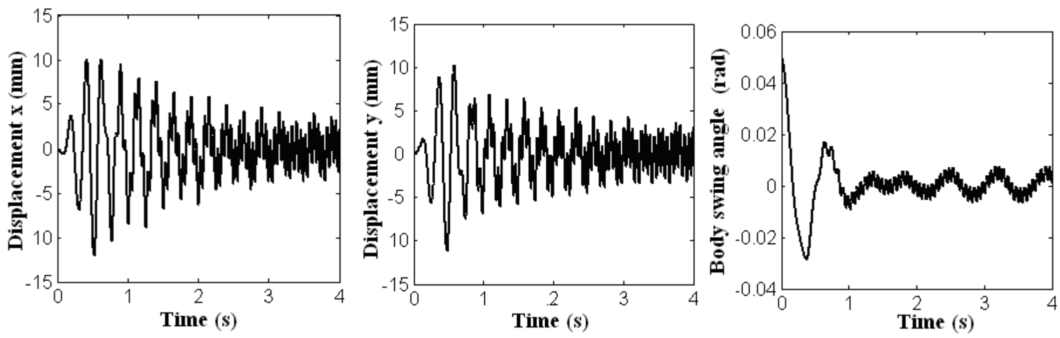

(d) Displacement *x* for $m_i r_i$ =0.4kgm (e) Displacement *y* for $m_i r_i$ =0.4kgm (f) Body swing angle for $m_i r_i$ =0.4kgm

Figure 3. Two cases with different exciter's eccentric moments.

3.2 The exciters' motor output torques

When the nominal torques of two exciter motors are the same as T_{N1}=T_{N2}=4, 3, 2 Nm respectively, the machine body can achieve self-synchronization after short transient time. Figure 4(a)~(b) are the motor output torques at T_{N1}=T_{N2}=2 Nm, and Figure 4(c)~(d) are the motor rotating speeds at the self-synchronous state. The simulated displacements in *x* and *y* directions of machine body are the same with those shown in Figure 3(a)~(b).

The simulated results show that, the bigger the exciters' motor output torques, the shorter the transient processing time for self-synchronization. Nevertheless, the nominal motor torques affect neither the vibration amplitude of stable synchronous movement of machine body, nor the motors' working torques and rotating speeds. After achieving a stable synchronous vibration, the exciters' motor output torques and their speeds will tend to be stable with only minor fluctuations around certain values.

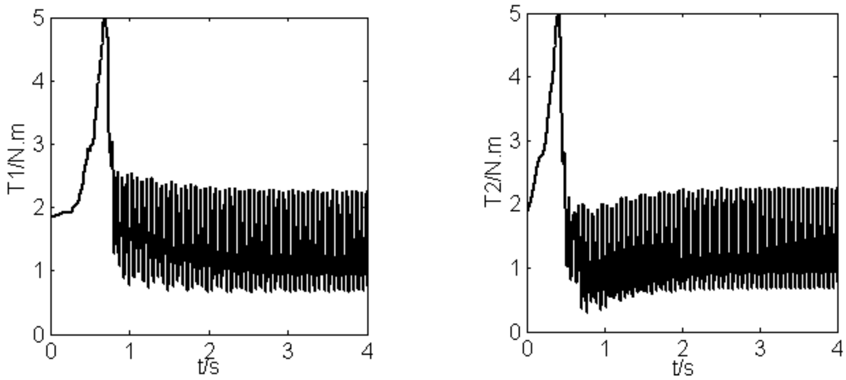

(a) Output torque of motor 1 (b) Output torque of motor 2

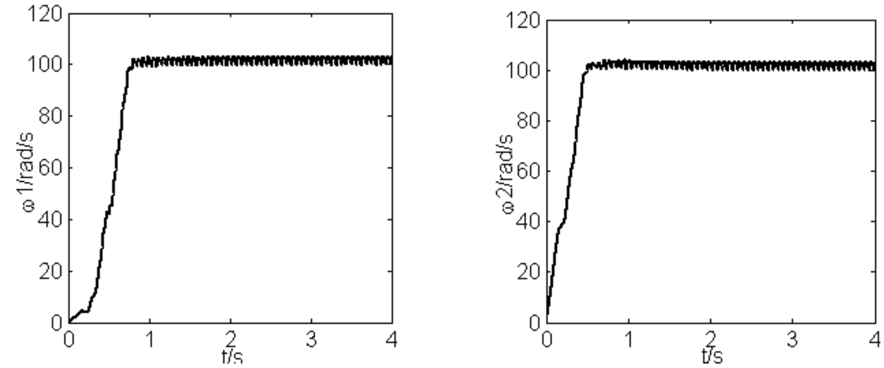

(c) Rotating speed of motor 1 (d) Rotating speed of motor 2

Figure 4 The synchronization case with exciter's motor nominal torques $T_{N1}=T_{N2}=2$ Nm

Furthermore, if the nominal motor torque decreases to a quite small value, such as 1Nm, the screener cannot achieve any synchronous movement at all, as shown in Figure 5, at $T_{N1}=T_{N2}=1$ Nm.

Figure 5(a)~(b) show the simulated displacement in *x* and *y* directions of the machine body with its transient processes. Figure 5(c)~(d) show the motor output torques in the state of non-synchronization. Figure 5(e)~(f) sow the rotating speeds of the two exciters changing greatly. The simulated body displacements, motor output torques and rotating speeds in Figure 5 are quite different from these of Figure 4.

It is obviously seen from Figure 5, for the non-synchronization due to lower motor torques, all vibrations of the machine body in *x*, *y* and ψ directions do not approach steady state even after a long time. The phase angle differences of two motors will keep on increasing.

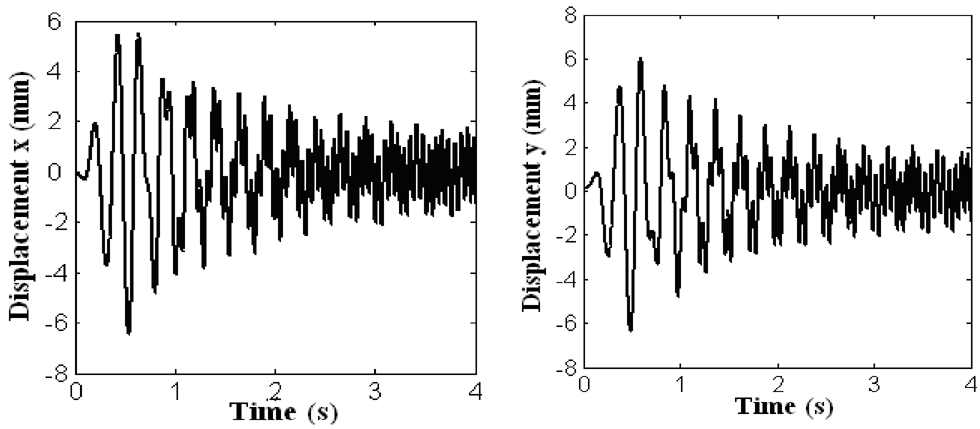

(a) Displacement in *x* direction (b) Displacement in *y* direction

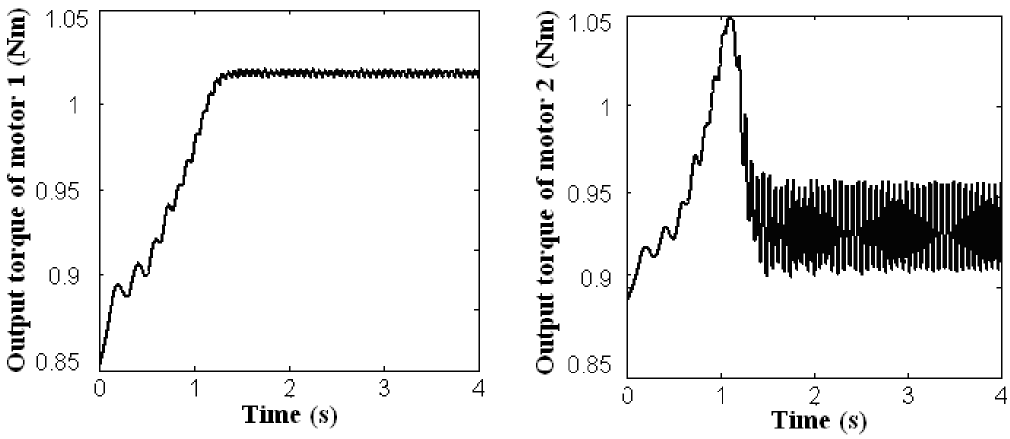

(c) Output torque of motor 1 (d) Output torque of motor 2

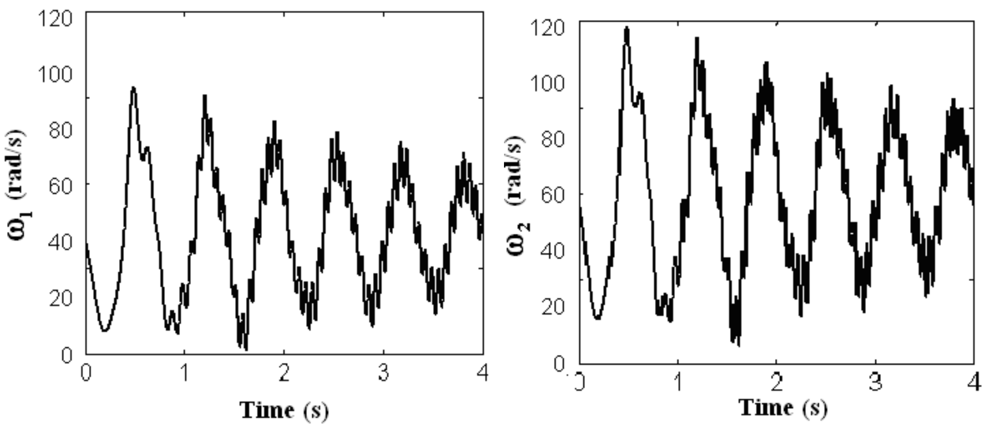

(e) Rotating speed of motor 1 (f) Rotating speed of motor 2

Figure 5. The non-synchronization case with exciter's motor torques T_{N1}=T_{N2}=1 Nm.

3.3 Simulations on synchronous transmission

As introduced in section 1, if one of the two exciters is switched off during the vibrating of the screener at its stable self-synchronization state, the screener motion can maintain its stable self-synchronous movement conditionally. The so-called synchronous transmission process is interesting for further understanding and will be investigated as follows.

A simulated synchronous transmission process is illustrated in Figure 6. In the simulation, all the parameters are the same with those in section 2.2. When one of the exciter motors is shut down, its output driving torque is set as 0. The 'switch off' time occurs at 8 seconds.

Figure 6(a) shows the displacement in x direction, Figure 6(b) is the spectra of displacement x, Figure 6(c) is the displacement in y direction, and Figure 6(d) is the spectra of displacement y.

As shown in Figure 6, the vibrating displacement amplitude in x direction of the body, 0.032mm, driven by two motors, (normal self-synchronization stage), is much smaller than the amplitude in y direction, 2.8mm. Their vibrating frequency in the two directions is identically the same to be 16Hz.

It is observed, at the switching point, the machine body displacements fluctuates for few seconds, and then resumes the stable synchronous movement. After that, the machine body vibrates at a frequency of 16Hz with different vibrating amplitudes obviously in both x and y directions.

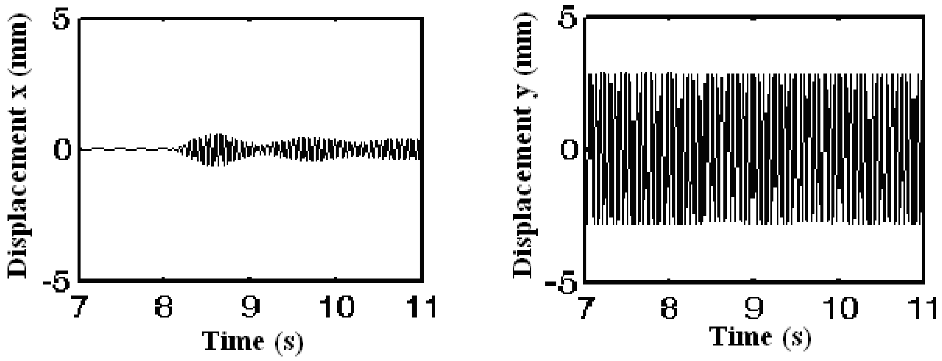

(a) Displacement in *x* direction (b) Displacement in *y* direction

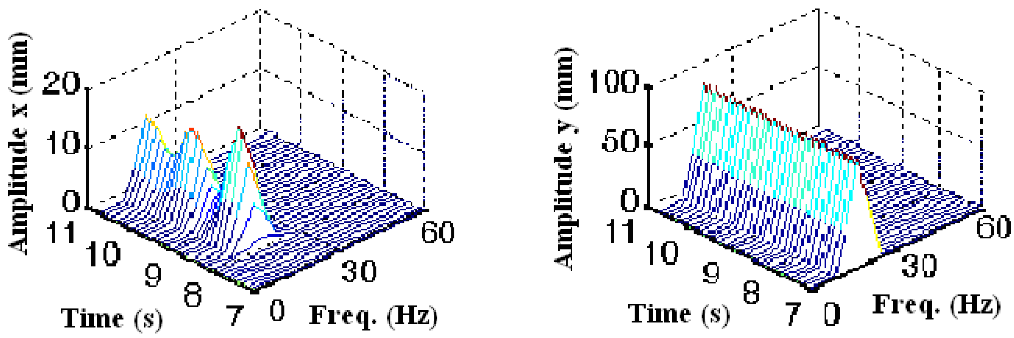

(c) Amplitude spectra of displacement x (d) Amplitude spectra of displacement y

Figure 6. Transient displacements and their spectra of machine body in synchronous transmission.

The exciters' motor output torques and rotating speeds, during synchronous transmission period, are simulated as shown in Figure 7. Figure 7(a)~(b) show the changing processes of the output torques of motor 1 and 2, while the motor 2 is shut down at 8 seconds. Figure 7(c)~(d) are the corresponding rotating speeds of the two exciters. It is shown the output torque of motor 1 increases about 0.1Nm and the rotating speeds of two motors decrease slightly and fluctuate obviously.

Actually, the increase of torque in motor 1 is the results of the energy transfer from motor 2 via the coupling of the vibrating body, and is necessary to overcome the resistant moments and to maintain synchronous motions.

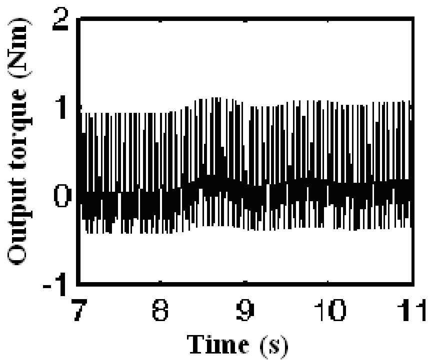

(a) Output torque of motor 1

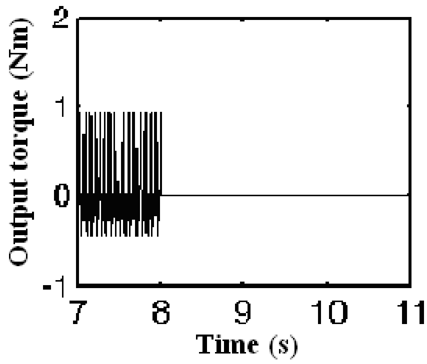

(b) Output torque of motor 2

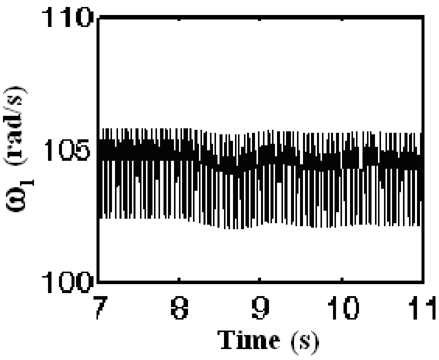

(c) Rotating speed of motor 1

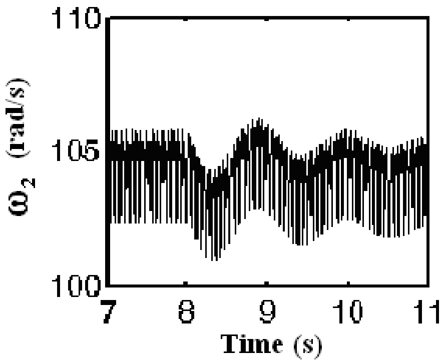

(d) Rotating speed of motor 2

Figure 7. Transient processes of motors output torque and rotating speeds in synchronous transmission.

Besides, the influences of eccentric mass moment, rotating damping and motor normal torque are found to be obvious on the process of synchronous transmission. For the vibratory screener discussed here, the three parameters' ranges for self-synchronization or synchronous transmission are summarized in Table 2 from simulation results. From Table 2, it can be seen that the parameter thresholds with only one motor are much narrower than those with two motors.

Table 2 Parameter ranges for self-synchronization and synchronous transmission

Cases	Eccentric mass moment		Rotating dampness		Motor torque	
	Lower limit	Upper limit	Lower limit	Upper limit	Lower limit	Upper limit
Driven by two motors	0.04	0.6	0	0.16	0.5	50
Driven by one motor	0.04	0.4	0	0.002	0.5	5

4 Conclusions

A dynamical model of a vibratory screener considering two exciters' motor characteristics is firstly introduced in this paper. The model is validated by experimental measurements of a machine body in Laboratory. Based on this model, numerical simulations are conducted to investigate the effects of different exciters' parameters on the self-synchronizations of the vibratory screener. The main conclusions are summarized as follows.

(1) The machine body's vibration displacements will increase when the exciters' eccentric moments increase; meanwhile, the transient period from rest to self-synchronization movements vibrations will be shortened.

(2) The motors' normal torques have obviously effect on the stable self-synchronous movements too. However, if normal torques are too small, the self-synchronous vibration of the machine body cannot be achieved.

(3) The transient process will be lengthened if the exciters' rotating frictions increase. In this case, the motor output torques and rotating speeds will decrease.

(4) The simulations show that the vibratory screener will develop into a process of synchronous transmission even when one motor is shut down during operations. In synchronization transmission, the output torque of the working motor increases to compensate and maintain the self-synchronous motion, whilst the shut-down motor remains the same rotating speed. As a result, the vibrating displacements of machine body in x direction increases slightly compared with that in the steady state of two motors. This observation is attributed to the coupling among the machine body and the two exciters in the screener.

Acknowledgement
This work is supported by the Key Project of Science and Technology of Chinese Ministry of Education (No: 108037), and the National Nature Science Funds of China (Granted No.10402008 and No.50535010). The authors also gratefully acknowledge the helpful comments and suggestions of the reviewers, which have improved the presentation.

References

[1] I. I. Blekhman, A. L. Fradkov, O. P. Tomchina, D. E. Bogdanov. Self-synchronization and controlled synchronization: general definition and example design, *Mathematics and Computers in Simulation*, 58(2002), 367-384.

[2] I. I. Blekhman, Synchronization in science and technology, 1988, ASME Press, New York.

[3] B. C. Wen, Z. Y. Zhao, D H Shu. Mechanical system's vibration synchronization and control synchronization, 2003, Scientific Publishing House, Beijing.

[4] W. L. Xiong, et al. Engineering characteristics and its mechanism explanation of vibratory synchronization transmission. *Chinese Journal of Mechanical Engineering*, 17(2004), 185-188.

[5] Q. K. Han, X. G. Yang, Z. Y. Qin, B. C. Wen. Nonlinear stability of synchronous transmission in vibration system, *The International Conference on Mechanical Transmissions*, 2006, Chongqing, China.

[6] H. Nijmeijer. A dynamical control view on synchronization, *Physica D*, 154 (2001), 219-228.

[7] A. Rodriguez-Angeles. Synchronization of mechanical systems, 2002, Technische Universiteit Eindhoven, Eindhoven.

[8] Q.K. Han and B.C. Wen. Stability and bifurcation of self-synchronization of a vibratory screener excited by two eccentric motors, *Advances in Theoretical and Applied Mechanics*, Vol. 1, 2008, no. 3, 107 – 119.

Received: May 7, 2008